

UC San Diego

UC San Diego Previously Published Works

Title

Mitigation of fast ions from laser-produced Sn plasma for an extreme ultraviolet lithography source

Permalink

<https://escholarship.org/uc/item/3pj8f18z>

Journal

Applied Physics Letters, 89(11)

ISSN

0003-6951

Authors

Tao, Y
Tillack, M S

Publication Date

2006-09-01

Peer reviewed

Mitigation of fast ions from laser-produced Sn plasma for an extreme ultraviolet lithography source

Y. Tao^{a)} and M. S. Tillack

Department of Mechanical and Aerospace Engineering, University of California, San Diego, 9500 Gilman Drive, La Jolla, California 92093-0438 and the Center for Energy Research, University of California, San Diego, 9500 Gilman Drive, La Jolla, California 92093-0438

(Received 17 April 2006; accepted 18 July 2006; published online 13 September 2006)

The authors present evidence of the reduction of fast ion energy from laser-produced Sn plasma by introducing a low energy prepulse. The energy of Sn ions was reduced from more than 5 keV to less than 150 eV nearly without loss of the in-band conversion from laser to 13.5 nm extreme ultraviolet (EUV) emission as compared with that of a single pulse. The reason may come from the interaction of the main pulse with preplasma instead of the full density solid surface. This makes it possible to use the full density Sn target in the practical EUV lithography source. © 2006 American Institute of Physics. [DOI: 10.1063/1.2349831]

Extreme ultraviolet (EUV) lithography (EUVL) is a leading candidate for the next generation lithography tools in the semiconductor industry to produce smaller and faster microchips with a feature size of 32 nm or less.¹ However, several challenges must be addressed before applying it to high volume manufacture (HVM); one of them is to develop an efficient, clean, and powerful EUV light source.² Laser-produced plasma has been one of the most promising EUV light source candidates. Because of the availability of optics, most of the efforts focus on in-band (2% bandwidth) 13.5 nm EUV light. Recently, efforts around the world have greatly improved the conversion efficiency (CE) from laser to in-band 13.5 nm light. For example, 3% CE has been demonstrated using a solid density Sn target.³ However, mitigation of heavy debris from the plasma remains a critical issue.² H, C, N, and O are also very critical to the collector optics due to the high duty cycle.

A large number of ions with several keV of kinetic energy could be generated in laser-produced Sn plasma under conditions favorable for efficient 13.5 nm EUV emission, and numerous neutral particles with sizes up to several tens of micrometers are produced by plasma expansion and recombination during the expansion. Low density Sn-doped plastic foam,^{4,5} Sn-doped water droplet targets,⁶ and fine Sn particles driven by gas puff have been investigated as mass-limited targets to mitigate Sn particles. However, extra C, O, and H ions with very high velocity are inherently generated from these targets. Conventional methods have individual limitations. For example, gas cannot stop large size debris and results in absorption of EUV light. Electric and magnetic fields inherently cannot mitigate neutral particles. To date, no existing technique can meet the requirements of a practical EUV lithography system for HVM.

Besides total yield, the ion energy is also important due to its impact on collector optic damage. The sputtering rate of optics induced by Sn ions strongly depends on the energy of the particles. If the kinetic energy of the particles can be slowed down to around 100 eV, the sputtering rate could decrease more than an order of magnitude as compared with that of ions above 1 keV.⁷ In addition, lower energy particles are easier to remove using conventional methods, such as

ambient gas, electric field, and their combination. In very recent time, increasing efforts to reduce the ion kinetic energy have been carried out. For example, Sn foil punched off by a laser-excited shock wave showed approximately ten times reduction in ion kinetic energy.⁸

Ion acceleration in laser-produced plasmas can be ascribed to free expansion of the plasma into vacuum. The plasma expansion is determined by the initial ion density profile and external energy source. It should be possible to control the ion kinetic energy by controlling the initial ion density profile. A prepulse is a convenient way to introduce a preformed particle density profile. Xe ion energy was reduced by a factor of ~ 10 in laser-produced Xe jet plasma with a prepulse.⁹

In this letter, we demonstrate more than 30 times reduction in Sn ion kinetic energy from laser-produced Sn plasma by introducing a low energy prepulse nearly without loss of in-band conversion efficiency as compared with single pulse. This is a higher reduction in Sn ion energy than all other existing methods. The likely reason comes from the interaction of the main laser pulse with the preplasma instead of the full density surface. This provides a simple and efficient way to control the particle energy in the applications of laser-produced plasma from solid target.

The experiments were carried out using two lasers. One is a picosecond neodymium doped yttrium aluminum garnet (Nd:YAG) laser (EKSPLA), which generates a 1.064 μm laser pulse with pulse widths from 130 to 600 ps, acting as the prepulse. The other is a 7 ns Nd:YAG laser producing a 1.064 μm laser pulse with an energy of 650 mJ at 10 Hz. This laser is used to heat the EUV plasma, called the main pulse hereafter. The two lasers are synchronized by a pulse delay generator (Stanford DG535), with a jitter less than 0.5 ns. The two pulses are combined into a collinear path by a cube polarizer and focused onto the surface of a target placed in a vacuum chamber at normal incidence by one shared planoconvex lens with a focal length of 300 mm. The focal spot diameters (full width at half maximum) of the main pulse and prepulse are 100 and 300 μm , respectively. The target is bulk pure Sn slab. Vacuum in the chamber can be pumped down to 10^{-6} Torr.

The ion energy spectrum was measured with a Faraday cup (FC) from Kimball Physics, which is placed at a distance of 15 cm from the plasma. The FC is biased with a -30 V

^{a)}Electronic mail: yetao@ucsd.edu

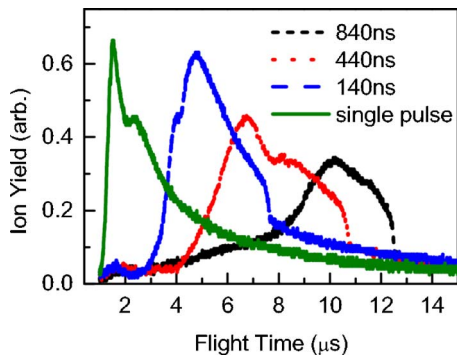


FIG. 1. (Color online) Typical time of flight profiles of Sn ions from laser-produced plasmas driven with a single pulse (green solid line) or with a dual pulse having various delay times of 140 ns (blue dashed line), 440 ns (red dotted line), and 840 ns (black short-dashed line).

voltage. The angular distribution of ions was measured by placing the FC at various angles from 10° to 90° with respect to the target normal. In-band CE was measured with a calibrated EUV energy monitor (E-mon) from Jenoptik, which consists of a Zr filter, two near-normal-incident multilayer Mo/Si mirrors, and an x-ray photodiode. The CE is integrated over a 2π solid angle. The E-mon is installed in the plane of laser incidence at an angle of 45° with respect to the target normal. The signals from both the E-mon and FC are recorded and processed with a digital oscilloscope.

Typical time of flight (TOF) data for Sn ions from laser-produced Sn plasma driven with single (solid line) and dual pulses at various delay times of 140, 440, and 840 ns (dashed lines) are shown in Fig. 1 (color online). The data were measured by the FC placed at 10° with respect to the target normal. The zero point represents the delay time in which the peaks of the pre- and main pulses overlap each other. The laser intensity of the main pulse is always 2×10^{11} W/cm 2 . The prepulse laser energy is 2 mJ. It is seen that in the case of a single pulse, most of the ions are located at times earlier than $4 \mu\text{s}$, and their flux peak is located at $1.7 \mu\text{s}$. However, using a prepulse with a delay time longer than 140 ns, a significant shift towards later time is seen. With delay time of 840 ns, the peak of the flux moves to $10 \mu\text{s}$.

The kinetic energy of ions at the peak flux as shown in Fig. 1 is calculated at various delay times using the kinetic energy formula $E = 1/2 m_i v^2$, where $v = d/t$ is the velocity of the ions, $d = 15$ cm is the distance from the plasma to the FC, and m_i is the atomic mass of Sn. The reduction factor of the ion kinetic energy obtained from dual pulse as compared with that obtained from a single pulse is shown in Fig. 2 (dots) (color online). When a prepulse is introduced with a delay time around 840 ns prior to the main pulse, the ion energy at the flux peak is reduced to less than 150 eV from higher than 5 keV obtained with a single pulse. More than 30 times reduction in ion kinetic energy is achieved.

In-band conversion efficiency was measured in the same shots as the ion TOF measurements. Typical results are plotted in Fig. 2 (squares) as a function of delay time. Each point represents the average of three shots. The in-band CE in the case of a single pulse, measured under the same conditions as the measurement for dual pulse except that the prepulse was blocked, is 2%. When the delay is less than 20 ns, there is an $\sim 10\%$ enhancement of CE as compared with a single pulse.

The enhancement of plasma emission by introducing a prepulse has been recognized for a long time.¹⁰ However,

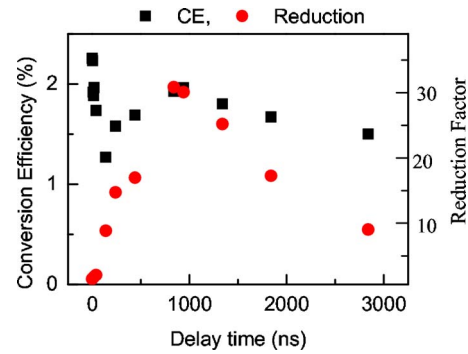


FIG. 2. (Color online) Reduction factor in ion kinetic energy at the flux peak (dots) and in-band conversion efficiency (squares) as a function of delay time between pre- and main pulses.

when the delay time is above 40 ns, the CE starts to drop and reaches a local minimum around 140 ns. After that, the CE recovers and reaches a value very close to that of a single pulse when the delay time ranges from 800 to 1200 ns. A lower CE is obtained with a delay time longer than 1200 ns. Recalling the measurement of ion energy, with a delay time around 800 ns, a large reduction in ion kinetic energy is obtained while almost the same in-band conversion efficiency is achieved as compared with that of a single pulse.

There are two possible mechanisms for the main pulse interaction with the target. One is that the main laser pulse passes through the low density preplasma and interacts with the full density target surface. The main plasma expands into vacuum, passing through the low density preplasma. The fast ions are slowed by collisions between the main and preplasmas. The stopping power of neutral gas can be simplified as¹¹

$$S = kZ_1 Z_2^2 L / \beta^2, \quad (1)$$

where $k = 0.3071/Z_2$ having units of keV/(mg/cm 2), Z_1 and Z_2 are atomic numbers of particle and ambient gas, respectively, L is the stopping number, and $\beta = v/c$ is the relative velocity of particles. Equation (1) predicts that gas is more effective at stopping slow ions rather than fast ions. However, recalling that fast ions are more efficiently stopped than slow ions in our case, this cannot explain our experiments.

The other possible mechanism is that most of the main laser pulse is deposited inside the preplasma and blocked from the solid target surface. It has been shown under very similar conditions that laser energy could be absorbed within a wide underdense plasma region in laser-produced Sn plasma rather than localized near the critical density.¹² Because the intensity of the prepulse, 2×10^{10} W/cm 2 , is above the threshold of phase explosion,¹³ the preplasma should include two plumes separated in time: One is well known as thermal plume occurring from the start of the laser pulse with an expansion velocity of 10^6 cm/s, the other is a cold plume due to the phase explosion appearing at several hundreds of nanoseconds after the laser pulse with an expansion velocity of 10^4 cm/s, called pre-cold-plume hereafter. When delay time is less than 20 ns, the main laser pulse mainly interacts with the thermal plume with a suitable density for efficient EUV generation; however, small reduction in ion energy is observed due to its steep density profile. When delay time is longer than 40 ns, the density of the thermal plasma becomes not high enough to generate efficient 13.5 nm EUV light, but it still blocks a significant energy of

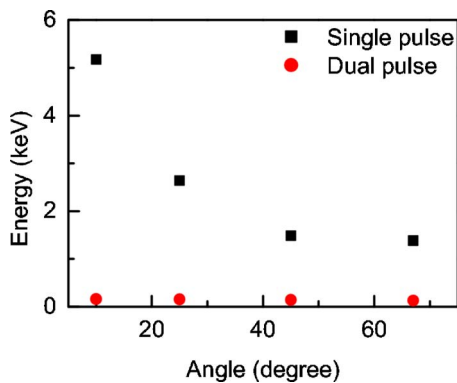


FIG. 3. (Color online) Angular distributions of ion kinetic energy at the flux peak with single (squares) or dual pulses (dots).

the main pulse, so lower CE is resulted, and the CE reaches its minimum at 140 ns. After that time, more energy of the main pulse can pass through the thermal plasma with less density, and the pre-cold-plume starts to appear in front of the target surface, the transmitted main pulse interacts with the pre-cold-plume instead of the full density surface. But at the times less than 800 ns, the density profile of the pre-cold-plume is still too steep, then CE starts to recover but the reduction in ion energy is still small. At delay times from 800 to 1200 ns, the thermal plasma should nearly disappear; and the pre-cold-plume forms a lower and smooth density profile. In this case, the plasma density is suitable for efficient 13.5 nm EUV generation, and the initial smooth ion density profile should result in inefficient ion acceleration in free expansion of the main plasma. So high CE and large reduction in ion energy are observed at these times. At longer delay time (>1200 ns), the density of the pre-cold-plume also becomes too low both to generate efficient 13.5 nm EUV light and to block all of the main laser pulse to reach solid target, so lower CE and small reduction in ion energy are resulted. In order to clarify this phenomenon completely, further plasma diagnostic and theoretical efforts need to be carried out.

The angular distribution of ion kinetic energy at the flux peaks with (squares) and without (dots) the prepulse is shown in Fig. 3 (color online). The laser intensity is constant at 2×10^{11} W/cm². The delay time is fixed at 840 ns. The prepulse energy is 2 mJ. In the case of a single pulse, a peak of ion energy appears at the target normal direction and the ion energy drops with increasing angle. However, the introduction of the prepulse results in an almost uniform angular distribution. This shows that this technique is effective at reducing the ion kinetic energy over the whole range of angles, but especially effective at small angles with respect to the target normal direction.

The effect of pulse duration was investigated by adopting 130–600 ps at the same conditions. It was noted that a short pulse is not necessary. But when a longer pulse is used, more energy is required to achieve high reduction factors. Lasers with pulse duration less than 20 ps and energy less than 1 mJ working at 100 kHz are commercially available and economical to operate. It is worthy to note that in our experiments the focal spot of prepulse is much larger than that of the main pulse. So the necessary energy of prepulse can be reduced further.

The kinetic energy of neutral particles from laser-produced plasma is also potentially reduced with the intro-

duction of a prepulse, because most of the energy of the neutral particles can be ascribed to the kinetic energy of ions.

The combination of this technique (dual pulse) with ambient gas or a gas-puff curtain makes it possible to use full density mass-limited Sn targets in an EUVL source for HVM. In that way, the kinetic energy of the particles from the plasma is reduced by the use of double pulse, then the slowed particles are mitigated by the gas or the gas-puff curtain.

To summarize, a technique based on dual-pulse irradiation is investigated to mitigate the fast ions from laser-produced Sn plasma. More than 30 times reduction in ion peak energy was obtained by introducing a 2 mJ prepulse laser. At the same time, in-band conversion efficiency from laser to 13.5 nm EUV emission is almost the same as that of a single pulse. The likely mechanism is the interaction of the main pulse with the preformed neutral particles having a lower density profile instead of the full density initial target surface. The technique is simple in experimental arrangement, and no large modification is necessary to couple it into existing laser systems. This also makes it possible to apply full density Sn targets to a practical EUVL source. In addition to an EUVL source, this result also provides an efficient and economical way to control the particle energy in the applications of laser-produced plasmas, such as pulsed laser deposition and soft and hard x-ray sources. Further experimental and theoretical efforts are being carried out to clarify the physics dominating the ion acceleration from the interaction of laser-produced plasma driven by a dual pulse.

¹P. J. Silverman, *J. Microlithogr., Microfabr., Microsyst.* **4**, 011006 (2005).

²U. Stamm, *J. Phys. D* **37**, 3244 (2004).

³Y. Shimada, H. Nishimura, M. Nakai, K. Hashimoto, M. Yamaura, Y. Tao, K. Shigemori, T. Okuno, K. Nishihara, T. Kawamura, A. Sunahara, T. Nishikawa, A. Sasaki, K. Nagai, T. Norimatsu, S. Fujioka, S. Uchida, N. Miyanaga, Y. Izawa, and C. Yamanaka, *Appl. Phys. Lett.* **86**, 051501 (2005).

⁴Keiji Nagai, QinCui Gu, ZhongZe Gu, Tomoharu Okuno, Shinsuke Fujioka, Hiroaki Nishimura, YeZheng Tao, Yuzuri Yasuda, Mitsuo Nakai, Takayoshi Norimatsu, Yoshinori Shimada, Michiteru Yamaura, Hidetsugu Yoshida, Masahiro Nakatsuka, Noriaki Miyanaga, Katsunobu Nishihara, and Yasukazu Izawa, *Appl. Phys. Lett.* **88**, 094102 (2006).

⁵S. S. Harilal, B. O'Shay, M. S. Tillack, Y. Tao, R. Paguio, A. Nikroo, and C. A. Back, *J. Phys. D* **39**, 484 (2006).

⁶M. Richardson, C. Koay, K. Takenoshita, C. Keyser, and M. Al-Rabban, *J. Vac. Sci. Technol. B* **22**, 785 (2004).

⁷Jean P. Allain, Ahmed Hassanein, Martin Nieto, Vladimir Titov, Perry Plotkin, Edward Hinson, Bryan J. Rice, R. Bristol, Daniel Rokusek, Wayne Lytle, Brent J. Heuser, Monica M. C. Allain, Hyunsu Ju, and Christopher Chrobak, *Proc. SPIE* **5751**, 1110 (2005).

⁸Shinsuke Fujioka, Hiroaki Nishimura, Tsuyoshi Ando, Nobuyoshi Ueda, Shinichi Namba, Tatsuya Aota, Masakatsu Murakami, Katsunobu Nishihara, Young-G. Kang, Atsushi Sunahara, Hiroyuki Furukawa, Yoshinori Shimada, Kazuhisa Hashimoto, Michiteru Yamaura, Yuzuri Yasuda, Keiji Nagai, Takayoshi Norimatsu, Noriaki Miyanaga, Yasukazu Izawa, and Kunioki Mima, *Proc. SPIE* **6151**, 61513V (2006).

⁹Hakaru Mizoguchi, Akira Endo, Tatsuya Ariga, Taisuke Miura, Hideo Hoshino, Yoshifumi Ueno, Masaki Nakano, Hiroshi Komori, Akira Sumitani, Tamotsu Abe, Takashi Suganuma, Georg Soumagne, Hiroshi Someya, Yuichi Takabayashi, and Koichi Toyoda, *Proc. SPIE* **6151**, 61510S (2006).

¹⁰R. Kodama, T. Mochizuki, K. A. Tanaka, and C. Yamanaka, *Appl. Phys. Lett.* **50**, 720 (1987).

¹¹J. F. Ziegler, *J. Appl. Phys.* **85**, 1249 (1999).

¹²Y. Tao, H. Nishimura, S. Fujioka, A. Sunahara, M. Nakai, T. Okuno, N. Ueda, K. Nishihara, N. Miyanaga, and Y. Izawa, *Appl. Phys. Lett.* **86**, 201501 (2005).

¹³Jun Ren, Xiaobo Yin, Sergei S. Orlov, and Lambertus Hesselink, *Appl. Phys. Lett.* **88**, 061111 (2006).